SILICON WAFER CHARACTERIZATION BY PCD TECHNIQUE AIMING OPTICAL SENSOR FABRICATION BASED ON PHOTOVOLTAIC TECHNOLOGY

N. Stem[1], C. A. S. Ramos[1], A. F. Beloto[2] and M. Cid[1]
[1]Lab. de Microeletrônica – Depto de Engenharia de Sistemas Eletrônicos,
Escola Politécnica da USP, São Paulo, Zip Code 05508-970, Brazil
nstem@lme.usp.br, mcid@lme.usp.br, cramos@lme.usp.br
[2] INPE, Lab. Associado de Sensores e Materiais, S. J. Campos, S. P.
Zip Code 12245-970, Brazil, beloto@las.inpe.br

Abstract

At this work crystalline silicon wafers are characterized by using the photoconductive decay technique (PCD). Two surface passivation techniques, thermal oxidation and phosphorus diffusion, allowed evaluating the bulk lifetime of the FZ silicon (25-30Ω.cm) and the quality of passivation. The experimental results were transposed to n^+p structure, rear passivated (SiO_2 layer), using initially FZ silicon with two different base resistivity (25-30Ω.cm) and 0.5Ω.cm. In sequence a lower cost silicon, typically employed in photovoltaic industry (Cz Silicon with 2-3Ω.cm base resistivity) was used. The implied open-circuit voltages were also characterized, showing values typically found in high efficiency silicon solar cells, about 670.8mV for FZ silicon wafers with 0.5Ω.cm, and from 652.5mV to 662.6mV for Cz Si with resistivities 2.5Ω.cm and 3.3Ω.cm, respectively. The developed photovoltaic sensors have a wide range of applications in industry.

Keywords: Rear passivated silicon solar cells, optical sensor, FZ and Cz silicon and simple fabrication process.

Introduction

The sensors based on photovoltaic technology present a wide range of applications, such as radiometers, position detection, counter systems and time registers in an industrial production line, among others.

On the other hand, the silicon solar cells have also presented an important participation between the alternative energy sources.

Focusing on the state of the art, the most prominent technology of photovoltaic devices based on silicon wafers is the rear passivated silicon solar cells, characterized by presenting the highest efficiencies allowing the usage of thinner wafers; and therefore, reducing the production cost [1].

Some examples of the available technology of rear passivated silicon solar cells are the Passivated emitter rear located contacts (PERL) [2], Random Pyramids Passivated Emitter Rear Contact (RP-PERC) [3], and LASER fired contact (LFC) [4] fabrication processes.

The PERL fabrication process is complex, involving ultra clean facilities, several steps of photolitography, double anti-reflection coating over inverted pyramids; and therefore, becoming a high cost technology.

However, RP-PERC and LFC are considered low cost processes. In the former, the anti-reflection coating is simpler, being composed by random pyramids and a single anti-reflection coating, thus decreasing the required photolitographic steps. The contacts of this structure are obtained by sintering aluminum dots on the rear surface. Meanwhile, the latter type of solar cells uses the LASER to open the holes on the rear SiO_2 and sintering aluminum at the same time. At this technology, the aluminum diffuses some monlayers on the presence of the LASER decreasing the recombination under the contacts [5].

In order to illustrate the weaker dependence of the rear passivated silicon solar cell efficiencies on the silicon wafer thickness some theoretical simulations were performed using the PC1D code and an optimized homogeneous Gaussian profile emitter.

The conventional fabrication processes, Al diffused [6, 7] and Al screen printed [8], were admitted to have: a) internal reflection, ρ_{int}= 86% and 95%; b) back reflection, ρ_b=56% and 61.5%; and c) effective rear recombination,

S_{eff}= 2050 cm/s and 600cm/s, respectively. Meanwhile, the rear passivated structures were divided into three groups: PERL [9], RP-PERC [3] and LFC [4,10,11], presenting ρ_{int}=95% and ρ_b=95% in each analyzed case. On the other hand the S_{eff} were supposed to be 50cm/s, 275cm/s and 200cm/s, accordingly.

Figure 1 presents a comparison between the reached efficiencies as function of the wafer thickness of conventional fabrication processes (screen printed Al and diffused aluminum over the whole rear surface) and rear passivated structures (RP-PERC, LFC and PERL), following the efficiency growing order.

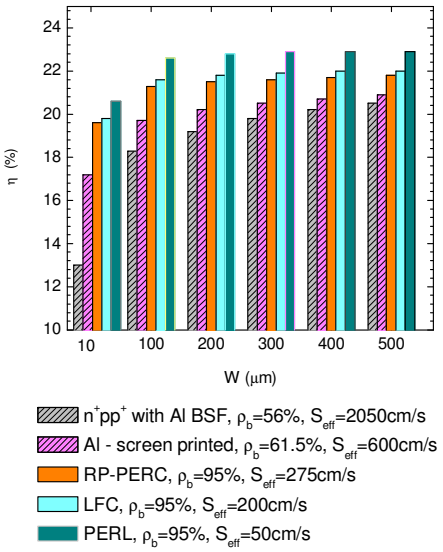

Fig. 1: The calculated efficiciencies as functions of the wafer thickness and technologies: the conventional ones (Al diffused and screen printed) and the rear passivated ones (RP-PERC [3], LFC [4, 10, 11] AND PERL [9]), assuming 2cm x 2cm area devices.

According to the figure 1, the highest efficiencies can be reached by PERL structures due to the p^+ regions under the rear contacts. The RP-PERC efficiencies are a bit lower than the ones presented by LASER fired contact solar cells.

However, the main distinction of these structures (RP-PERC, LFC and PERL) from the conventional ones (screen printed Al and Al diffused) is the fact that the rear passivated solar cell efficiencies present a non-significant decrease for thinner wafers, reducing the fabrication costs, as commented previously.

Thus, aiming to develop optical sensors with reduced costs, this work is focused on developing the required steps of the fabrication process of silicon solar cells with rear passivation using low resistivity Cz silicon and non-ultra cleaning facilities.

Photoconductive decay technique (PCD)

This technique is a contactless, being able to measure the effective minority carrier lifetime, τ_{eff} as function of the excess carrier density Δn, generated by an optical excitation, being widely used for monitoring solar cell fabrication processes, starting material characterization, etc.

Aiming to extract some information about the bulk lifetime in the analyzed sample, it is imperative to minimize the surface recombination velocity by passivating the surfaces, either using chemical passivation [12], thermal oxidation [13, 7, 14], phosphorus diffusion (n^+pn^+ structures) [15, 16, 7] or silicon nitride [17].

Analyzing surfaces passivated by thermal oxidation, the measured effective lifetime, τ_{eff}, is known to be dependent on frontal and rear surface recombination velocities, $2S_{eff}$, sample thickness, W, and bulk lifetime, τ_{bulk}, as seen in (1).

$$\frac{1}{\tau_{eff}} = \frac{2S_{eff}}{W} + \frac{1}{\tau_{bulk}} \qquad (1)$$

On the other hand, surfaces passivated by phosphorus diffusion can also provide information about the emitter recombination current density, J_{oe} of the structure n^+pn^+ with N_A dopant concentration and W thickness base, as shown by (2).

$$\frac{1}{\tau_{eff}} = \frac{1}{\tau_{bulk}} + \frac{2J_{oe}(\Delta n + N_A)}{qWn_i^2} \qquad (2)$$

At this work two kinds of surface passivation were used to characterize silicon: thermal oxidation over p-type silicon and n^+pn^+ structures, in each studied case a hydrogenation technique (alneal) was used after the thermal oxidation. In order to characterize material and fabrication process steps, p-type FZ silicon wafers with 25-30Ω.cm resistivity were chosen. The wafers with polished surfaces were cut into samples with 3cm x 3cm area, followed by the standard RCA cleaning. The obtained structures were applied in the fabrication process of rear passivated silicon solar cell using low resistivity materials (FZ and Cz).

Surface Characterization

The SiO_2 – Si – SiO_2 samples were oxidized using chlorinated compounds in open tube furnaces, and then characterized by PCD technique.

Figure 2 shows the measured effective lifetime of one of the most representative sample, E-6-5, presenting about 1ms for $\Delta n=N_A=5.4x10^{14}$ cm^{-3} (after alneal). A lower bound of the bulk lifetime, τ_{bulk} could be estimated at 1.01ms and a upper bound surface recombination velocity of about 13.6cm/s, proving the high quality of the starting material and the surface passivation, since they represent the minimum τ_{bulk} and the maximum S_{eff} that can be associated to this measurement, accordingly.

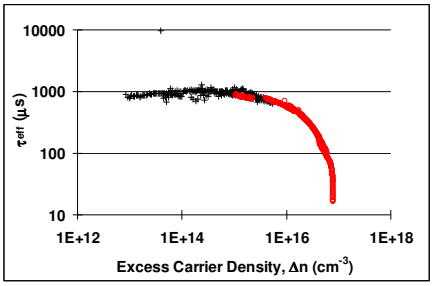

Fig. 2: Measured effective lifetime, $\tau_{eff}(\mu s)$ as function of the excess carrier density, $\Delta n(cm^{-3})$ considering the sample E-6-5 with the structure: SiO_2/p-type silicon/SiO_2.

At the same time, the phosphorus diffusion to obtain the n^+pn^+ structures were performed using $POCl_3$ source and aiming Gaussian profile emitters with about 100Ω/sq sheet resistance at the end of the process. In sequence, the samples had the PSG removed and were oxidized in the same way as described above.

Figure 3 shows the measured τ_{eff} (just after alneal) in one of the processed samples, E-17-6, with a 130Ω/sq emitter and a 28Ω.cm base. The orange curve represents a calculated τ_{eff} limit considering the J_{oe} component as the dominant one.

At this sample, the τ_{eff} for $\Delta n=N_A$ was about 1.2ms; therefore, showing that a high quality surface passivation could also be obtained over n^+-type Si, beside having the material τ_{bulk} preserved even after an increase in the thermal budget of the process.

Another remarkable point is that the obtained emitter could provide a low J_{oe}, about $45fA/cm^2$, as demonstrated by the orange curve in figure 3.

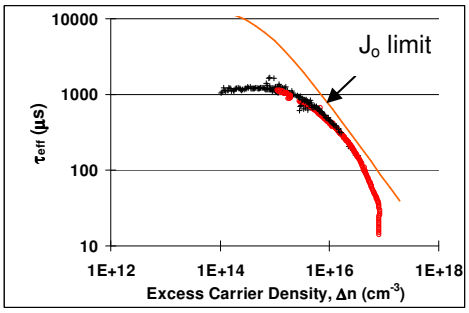

Fig. 3: Measured effective lifetime, τ_{eff} (μs) as function of excess carrier density, Δn (cm^{-3}) of the sample E-17-6, with the n^+pn^+ stucture.

After proving the high quality of surface passivation, over n^+-type and p-type silicon, silicon solar cells with n^+p structure and rear passivated using FZ and Cz silicon wafers (a lower cost material) were processed.

Rear passivated n^+p structures

Among the requirements that have to be satisfied in order to achieve high efficiencies in the rear passivated silicon solar cells are: to maintain the minority carrier bulk lifetime at suitable values for solar cell application, τ_{bulk}, aiming to obtain a high quality surface passivation over p-type (rear) and n^+-type silicon (front) and to process Gaussian profile and optimized emitters (surface doping levels and thicknesses).

The FZ and Cz silicon samples with 3cm x 3cm area were oxidized in chlorinated environment, and then submitted to a photolitographic step, resulting a $4cm^2$ useful frontal area. In sequence, the emitters were obtained by phosphorus diffusion, processed similarly to the ones in n^+pn^+ structures.

The emitter and base characteristics of the most representative samples are presented at table 1.

The emitters presented Gaussian profile and were optimized considering homogeneous emitters, characterized by having the same surface doping level under passivated and metal-contacted regions. The maximum theoretical efficiencies were obtained for the surface doping level range, $N_s=2x10^{19}cm^{-3}$ - $4x10^{18}cm^{-3}$ with the corresponding thickness range, W_e, ($0.5\mu m<W_e<1\mu m$) and ($1\mu m<W_e<3\mu m$) [17].

Table 1: Sample characteristics: base resistivity, emitter sheet resistance and surface doping level. Emitter thicknesses were about 2.0μm for all the samples.

sample	ρ (Ω.cm)	R_{sq} (Ω/sq)	N_s (cm^{-3})
E-14-5 (FZ)	28.2	180	$2.00x10^{18}$
B-23-4 (FZ)	0.5	55	$1.24x10^{19}$
A-22-2 (Cz)	2.5	55	$1.24x10^{19}$
5-2 (Cz)	3.3	101	$3.87x10^{18}$

The only exception was the sample E-14-5, where an optimized double diffused emitter was considered, whose optimized emitter surface doping level and thickness ranges are ($1x10^{18}cm^{-3}<N_s<1x10^{19}cm^{-3}$) ($0.5\mu m<W_e<10\mu m$) under the passivated region [17].

This type of emitter is characterized by presenting a higher surface doping level under the metal contacted regions. Thus, the n^+p structure of these samples was chosen to have the optimized emitter sheet resistance of its passivated region.

The PCD characterizations were performed after each thermal step, allowing the analysis of both, the effective lifetimes and the associated implied open-circuit voltages, $V_{oc\text{-}imp.}$.

The measured effetive lifetimes of the most representative samples after each thermal step considering 1 Sun operation point and intrinsic carrier concentration $n_i=1x10^{10}$ cm^{-3} are presented at table 2.

Table 2: The measured effective lifetimes after the thermal steps: oxidation, P pre-deposition and oxidation followed by alneal, considering 1 Sun operation point.

sample	oxidation (ms)	P pre-deposition (ms)	oxidation +alneal (ms)
E-14-5	0.300	0.120	0.475
B-23-4	0.016	0.020	0.089
A-22-2	0.063	0.068	0.245
5-2	0.121	0.026	0.347

According to table 2, despite the decrease in the lifetimes of some samples after phosphorus pre-deposition, they can be surpassed after the PSG dropping out followed by oxidation and alneal, due to the high quality of surface passivation of the developed process.

Figure 4 shows the measured effective lifetimes as functions of the excess carrier concentration of four of the most representative samples of the developed process, following the sequence B-23-4 (FZ sample with 0.5Ω.cm), A-22-2 (Cz sample with 2.5Ω.cm), 5-2 (Cz sample with 3.3 Ω.cm) and E-14-5 (FZ with 28.2 Ω.cm). The dashed lines represent the 1 Sun operation points as functions of the excesss carrier concentration for each represented sample.

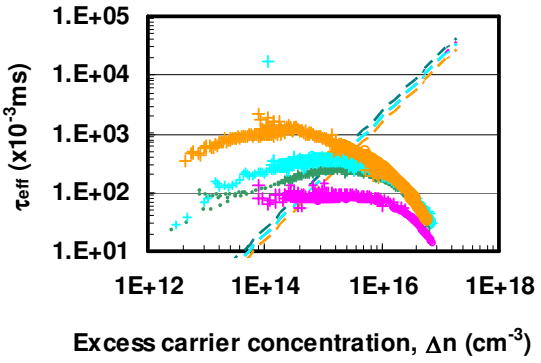

Fig. 4: Measured effective lifetime, τ_{eff} (ms) as function of the excess carrier concentration, Δn (cm^{-3}) at samples with the structure n^+p just after alneal. The growing sequence of τ_{eff} was adopted: B-23-4 (0.5Ω.cm), A-22-2 (2.5Ω.cm), 5-2 (3.3Ω.cm) and E-14-5 (28.2Ω.cm).

The implied open-circuit voltages, $V_{oc\text{-}imp}$ obtained just after alneal were also analyzed at the operation point of solar cells, as shown in figure 5.

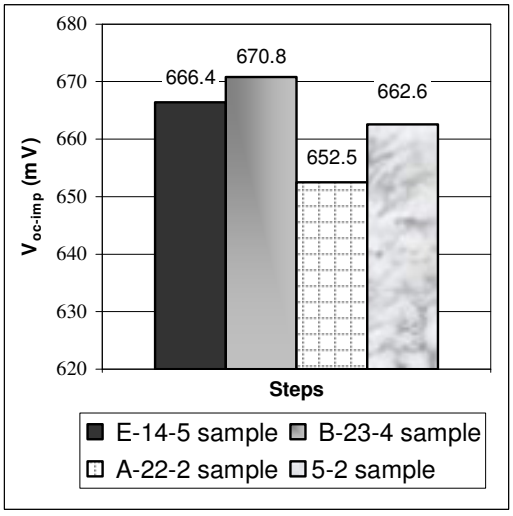

Fig. 5: The implied open-circuit voltages measured just after alneal at the samples with n^+p structure considering 1 Sun operation point.

Analyzing figure 5, it can be realized that high implied open-circuit voltages could be reached using different types of silicon, FZ and Cz, and base resistivities. This fact demonstrates that the quality of the surface passivation and the maintenance of the bulk lifetime could be assured in complete structures; and therefore, the possibility of developing rear passivated solar cells using industrial like facilities.

However, in order to obtain complete devices, the base resistivity needs to be taken into account. The highest contact resistance between the rear aluminum dots is associated to the bases with the highest resistivities, imposing the usage of rear locally doped contacts, as in PERL technology. Thus, a sample with the same structure of E-14-5 one (FZ silicon) could become a high efficient device if it were adopted a double-diffused emitter and locally doped rear contacts in the fabrication process. On the other range this structure can also be considered as a precursor of bifacial silicon solar cells, only requiring the development of a higher doped p-type region.

Meanwhile, the B-23-4 sample, by having only 0.5Ω.cm base resistivity, could provide high efficiencies with the RP-PERC structure.

Concerning the Cz silicon wafers, a low cost material, high efficiencies could be achieved by joining the LFC fabrication process to the RP-PERC one [10], and consequently obtaining high efficiencies even using wafers with typical industrial resistivities (1-3Ω.cm).

Efficiency predictions of low resistivity silicon wafers

Theoretical predictions with the PC1D program code of the efficiencies of the Cz and FZ samples with low resistivity (B-23-4, A-22-2 and 5-2) were performed, considering a typical frontal surface recombination velocities for an anti-reflection system composed by random pyramids plus SiO_2 layer (S_f=3000cm/s) [18], the measured effective lifetimes from table 2 and the emitter parameters from table 1. Some predictions, considering a double layer anti-reflection coating, were also performed.

According to the results, the theoretical efficiencies for samples B-23-4 (FZ Si with 0.5Ω.cm), A-22-2 (Cz Si with 2.5Ω.cm) and 5-2 (Cz Si with 3.3Ω.cm) were η=20.0%–20.2%, η=19.4%–19.7% and η=19.7%–20.0%, respectively. These values are comparable to the ones experimentally reached by other works [19, 20, 3], since a single layer of SiO_2 over random pyramids is considered as the frontal anti-reflection coating system and LASER fired contacts are adopted for the lowly doped bases.

On the other hand, if a double layer coating of ZnS/MgF_2 is adopted, the efficiencies of the FZ Si with 0.5Ω.cm sample could surpass 21% and the Cz ones could reach about 20%, even processing the devices in a non-ultra clean facility, as in the industrial ones.

Conclusions

High quality surface passivation over p-type and n^+-type silicon has been achieved due to the fabrication process optimization. The measured effective lifetimes showed that a high bulk lifetime could be associated; and therefore, being of interest for solar cell application.

For instance, the FZ Si with 0.5Ω.cm sample, B-23-4 (55Ω/sq emitter) provided open-circuit voltage of about 670.8mV at one Sun operation point. The samples A-22-2 (with a 55Ω/sq emitter and 2.5Ω.cm base) and 5-2 (with a 101Ω/sq emitter and 3.3Ω.cm base) presented $V_{oc\text{-}imp}$=652.4mV; and $V_{oc\text{-}imp}$= 662.6mV, respectively, considering 1Sun operation point.

If a typical low cost anti-reflection system (SiO_2 film over random pyramids) were considered, theoretical efficiency predictions for a device with similar characteristics could be about 20%. However, if a double layer (MgF_2-ZnS) were considered instead; the efficiency in the Cz silicon samples could surpass 20% and FZ Si with 0.5Ω.cm resistivity could achieve the mark of 21%.

Thus, the developed process can allow the obtaining of high efficiencies and at the same time the reduction of costs. This fact is mainly due to the introduction of rear passivation, making possible fabricate thinner samples without decreasing the achievable efficiencies.

References

[1] R. M. Swanson, Progress in Photovoltaics: Research and Applications, Vol. 14, pp. 443-453, 2006.

[2] J. Zhao; A. Wang and M. Green, Solar Energy Materials and Solar Cells, Vol. 66, pp. 27-36, 2001.

[3] S. W. Glunz; J. Knobloch; C. Hebling; W. Wettling, In proceedings of 26th PVSC, Anaheim, CA, pp. 231-234, 1997.

[4] E. Schneiderlochner; G. Emanuel; G. Grupp; H. Lautenschlager; A. Leimenstoll; S. W. Glunz; R. Preu and G. Willeke, in the Proceedings of 19th European Photovoltaic Solar Energy Conference, Paris, France, CD-ROM, 2004.

[5] Schneiderlöchner, E; Grohe, A.; Balif, C.; Glunz, S. W.; Preu, R. And Willeke, G., in proceedings of the IEEE 29th Photovoltaic Specialists Conference, New Orleans, Lousiana, pp. 300-303, 2002.

[6] R. Lago-Aurrekoetxa; C. del Cañizo; I. Tobias and A. Luque, Solid state electronics, Vol. 49, pp. 49-55, 2005.
[7] N. Stem, Células solares de silício de alto rendimento: otimizações teóricas e implementações experimentais utilizando processos de baixo custo, PhD thesis submitted to Escola Politécnica da Universidade de São Paulo, 2007,http://www.teses.usp.br/teses/disponiveis/3/3140/tde-02042008-113959/
[8] A. Rohatgi; S. Ebong; M. Hilali; V. Meemongkolkiat; B. Rousaville and A. Ristow, in Proceedings of 15th PVSC, China, CD-ROM, 2005.
[9] A. Aberle; W. Warta and J. Knobloch and B. Voβ, 21st IEEE Photovoltaic Specialists Conference, pp. 233-238, 1990.
[10] R. Preu; E. Schneiderlochner; A. Grohe; S. W. Glunz and G. Willeke, in proceedings of 29th IEEE Photovoltaic Specialists Conference, pp. 130-133, New Orleans, Lousiana, 2002.
[11] E. Schneiderlochner; R. Preu; R. Ludemann and S. W. Glunz, Progress in Photovoltaics: Research and Applications; Vol. 10; pp. 29-34, 2002.
[12] R. Lago; I. Tobias; C. Del Cañizo and A. Luque, Journal of The Eletrochemical Society, Vol. 148, nº 4, pp. G200–G206, 2001.
[13] N. Stem; E. G. Moreira; M. Cid; C. A. S. Ramos and M. Vasconcelos, in Proceedings: International Nuclear Atlantic Conference 2007 (XV ENFIR and XVII ENAN), Santos – S.P, CD-ROM, 2007.
[14] Kerr, M. J. Surface, emitter and emitter recombination and development of silicon nitride passivated solar cells. 2002. PhD thesis submitted to The Australian National University, Australia, 2002.
[15] A. Cuevas, Solar Energy Materials & Solar Cells, Vol. 57, pp. 277-290, 1999.
[16] C. A. Ramos; N. Stem and M. Cid, in Anais I Congresso Brasileiro de Energia Solar (I CBENS), 8 a 11 de abril de 2007 em Fortaleza, Brasil, CD-ROM.
[17] N. Stem; M. Cid and A. Cuevas, in Proceedings of 21st European Photovoltaic Solar Energy Conference, Dresden, Germany, pp. 439-442, 2006.
[18] P. P. Altermatt; J. O. Schumacher; A. Cuevas; M. J. Kerr; S. W. Glunz; R. R. King; G. Heiser; A. Schenk, Journal of Applied Physics, Vol. 92, nº 6, pp. 3187–3197, 2002.
[19] S. H. LEE, Journal of the Korean Physical Society, Vol. 39, nº 2, pp 369-373, 2001.
[20] B. Fischer; M. Keil; P. Fath; E. Bucher, in the Proceedings of 17th European Solar Energy Conference Exhibition, Munich, Germany, CD-ROM, 2001.

Acknowledgements

N. Stem was supported by a CNPq scholarship under the process nº 141460/2000-8.